

# CHARACTERIZATION OF NON-CRIMP FABRICS FOR PREFORMING SIMULATION

Bae, J<sup>1,2</sup>, Khoun, L<sup>3</sup>, Trudeau, P<sup>3</sup> and Hubert, P<sup>1,2\*</sup>

<sup>1</sup> Department of Mechanical Engineering, McGill University, Montreal, Canada

<sup>2</sup> Centre de Recherche sur les Systèmes Polymères et Composites à Haute Performance, Montreal, Canada

<sup>3</sup> Automotive and Surface Transportation Centre, National Research Council Canada, Boucherville, Canada

\* Corresponding author (pascal.hubert@mcgill.ca)

**Keywords:** *preforming, non-crimp fabrics, simulation*

## ABSTRACT

The objective of this paper is to characterize the drapability properties (shear and bending) of non-crimp fabrics (NCF) and to implement the measured material properties into PAM-FORM software to carry out preforming simulations. The picture-frame method (ASTM D8057) and the bending cantilever test by Peirce (modified from ASTM D1388) were used to characterize NCF shear and bending properties, respectively. Methodology was developed to ensure test reproducibility. The characterized reinforcement properties were implemented as material data card of the PAM-FORM software. The material data cards were validated by modelling the picture-frame test and the bending cantilever characterization tests in PAM-FORM. Good correlations were achieved between the simulation data and the measured experimental data.

## 1 INTRODUCTION

The automotive and aerospace industries are constantly looking for improvements in their manufacturing techniques to decrease the manufacturing cost. Liquid Composite Moulding processes (LCM) using non-crimp fabrics (NCF) is seen as an economical option. NCF are known to have great drapability properties which increase their potential use in terms of design and geometry flexibility. They also have higher mechanical properties than woven fabrics as they are constructed without weaves. Furthermore, due to the simpler yarn construction NCF manufacturing cost is more economical compared to woven fabrics. However, NCF are more difficult to manipulate due to their structural instability. They are prone to fraying at the edge and shear more freely as they are usually only held by stitches [1]. Those disadvantages make accurate material characterization more difficult and increase variability of the fabric drapability behaviour [2].

In the past decades, preforming simulation tools have been developed to predict the preforming capabilities of dry fabrics as well as thermoset and thermoplastic pre-impregnated (prepreg) materials. Preforming simulations are used to predict preforming defects such as wrinkling, bridging, thickness variation, or shear at both ply and laminate levels. Defects are often caused by a combination of several different factors such as material properties and boundary conditions. Simulation tools can also determine the final fibre orientation and the shear angle which are critical for local mechanical strength and local permeability [3, 4]. There are three different categories of preforming simulations: kinematic mapping, mesoscopic finite element modelling (FEM) and macroscopic FEM. Macroscopic FEM simulation with refined mesh gives a reasonably good prediction of the local shear angle prediction with less than 10° of difference compared to experimental preforming [5]. However, it relies highly on the material experimental characterization data [5]. Thus, an accurate characterization methodology is crucial for a macroscopic

simulation to give accurate results [6]. The macroscopic FEM was widely used for woven fabrics, but not many studies were performed on NCF despite its mechanical and economical advantages [7]. The material behaviour in shear, bending and tensile loading is required to conduct macroscopic preforming simulations for NCF. Additionally, the friction behaviour between fabric layers and between the tool material and fabrics need to be measured.

The shear behaviour is the most important deformation mode in dry fabric preforming as it determines the final fibre direction [8]. There is no simple relationship between shear angle and wrinkling [9]. From the literature both picture-frame and bias-extension tests are often performed to measure this property [7, 10]. The picture-frame test prevents sliding of the fibres, but it must be performed with more care as it is sensitive to fibre alignment [10]. Several studies have shown that some NCF can have asymmetric shear behaviour depending on their architecture and stitch pattern [2, 11].

The out-of-plane bending behaviour is the second most important factor in the deformation of the fabrics. Although wrinkles depend on several factors such as strain levels, stiffness, and boundary conditions, bending stiffness is the most important factor for wrinkles formation [9, 12]. It has been shown that higher bending rigidity increases wrinkle formation [9]. The methodology to measure the out-of-plane bending stiffness is the cantilever bending test following ASTM D1388. This test consists of increasing the overhang length gradually until the tested sample strip reaches 41.5°. One of the drawbacks of ASTM D1388 is that it is limited to a single bending angle. Bilbao et al. [13] used this cantilever test with various overhang lengths to determine the bending modulus as a function of the radius of curvature and characterize non-linear and non-elastic bending behaviour.

The tensile behaviour is not as important as the shear or bending behaviour in fabric deformation, but it is critical if there is a blank holder in the preforming setup as it applies tension into the fabrics [9]. Finally, the friction coefficient between each ply and between the tool and the fabric can vary between 0.1-0.5 [14]. In several studies, friction coefficients have been assumed to be 0.2 [9, 12].

Proper characterization methodologies are required to create accurate preforming simulation. In the literature, dry fabric characterization tests are well defined for woven fabrics but not well for NCF architectures [7]. Thus, the objective of the present work is to characterize the shear and bending behaviour of NCF and develop models that can be implemented in a commercial macroscopic FEM preforming simulation tool (PAM-FORM).

## 2 MATERIALS AND METHODOLOGY

### 2.1 Materials

Glass fibre NCF studied in this paper (TG15N, TG33N, SG33N) were supplied by Texonic <sup>Inc.</sup> Table 1 summarizes the main fabric properties. The NCF contains one layer of UD glass fibres in the warp direction stacked between two layers of glass fibres in the weft direction. The layers are stitched with a thin polyester yarn in the warp direction. SG33N and TG33N have the same architecture with a higher areal density compared to TG15N. SG33N also contains thermoplastic stitches in the warp direction, which can be used as in-situ binder for the preforming and eliminate the powder binder application step.

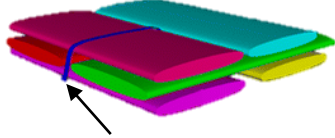
Table 1. Technical data sheet information of the suited NCF [15-17].

Material	TG15N	SG33N	TG33N
Infused Thickness (mm)	0.45	0.75	0.86
Aerial Weight (g/m <sup>2</sup> )	518	1135	1125

Illustration





Stitch

[18]

Stitch Composition (Warp Direction)	Polyester	Polyester+ Thermoplastic binder	Polyester
Warp/Weft Weight Ratio	44%-56%	46%-54%	45%-55%
Warp Material Composition	735 tex (GF) 16.77 tex (Polyester) 3.1/cm	1100 tex (GF) 16.66 tex (Polyester) 60 tex (UniFlex™) 4.6 /cm	1100 tex (GF) 16.66 tex (Polyester) 4.6 /cm
Weft Material Composition	275 tex (GF) 10.4 /cm	735 tex (GF) 8.4 /cm	735 tex (GF) 8.4/cm

## 2.2 Picture-Frame Test Methodology

Picture-frame (also known as trellis-frame) tests were performed on an Instron® 5985 testing machine with a 5 kN load cell. The samples (minimum of three) were clamped at the edges of a four-corner pinned jig (see Figure 1-a) in order to prevent slippage. The samples were loaded in tension with a constant displacement rate causing the shearing of the reinforcement as depicted in Figure 1-b. A crosshead speed of 20 mm/min was selected. Samples were tested in both positive (+45°) and negative (-45°) shear angle with respect to the warp orientation, to determine if there was a difference between the warp and weft direction of the fabric. Figure 2 shows the sample placed in the picture frame with the two possible orientations.

The shear stress ( $\tau$ ) and strain ( $\gamma$ ) were calculated using Equations (1) and (2) [4, 19]:

$$\tau = \frac{2 \cdot F_x \cdot \left(\frac{h+d/2}{L}\right)}{T_h \cdot L} \quad (1)$$

$$\gamma = \frac{\pi}{2} - 2 \cdot \cos^{-1} \left( \frac{h+d/2}{L} \right) \quad (2)$$

where  $F_x$  is the applied load,  $T_h$  is the thickness of the fabric,  $L$  is the length of side of the picture frame,  $d$  is the crosshead displacement and  $h$  is the length of the side adjacent to the angle, as show in Figure 1-c.

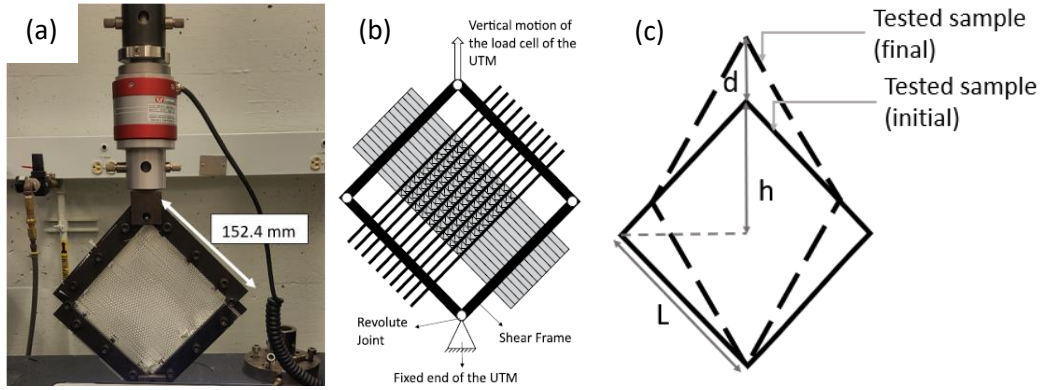


Figure 1. (a) Picture-frame setup, (b) schematic of the picture frame setup [20] and (c) geometrical parameters.

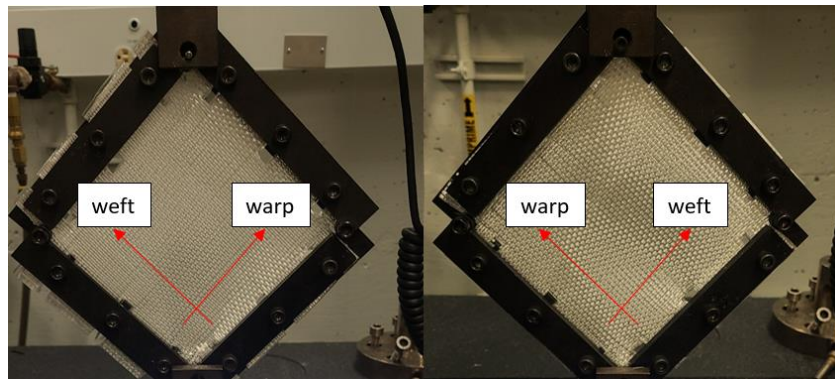


Figure 2. Sample orientation: (left) positive shear angle and (right) negative shear angle

### 2.3 Bending Cantilever Test Methodology

The cantilever bending test (modified from ASTM D1388) was performed to measure the fabric bending behaviour with Taber® Fabric Stiffness Tester. A schematic of the test is illustrated in Figure 3. The samples width was 2.54 mm and three overhang lengths (80mm, 110mm, 130mm) were tested. Both bending properties along warp and weft directions were measured. For each sample, a side view picture of the specimen was taken. The sample deflection ( $\delta$ ) and the curvature profile were analyzed using “GetData Graph Digitizer” [21] image analysis software. The flexural rigidity ( $G$ ) and bending modulus ( $B$ ) were calculated using the following equations [13, 22]:

$$G = g \cdot \rho_A \cdot c^3 \quad (3)$$

$$B = 12 \cdot \frac{G}{T_h^3} \quad (4)$$

with

$$\rho_A = \rho \cdot T_h \quad (5)$$

$$c = OL \cdot \left( \frac{\cos(\theta/2)}{8 \cdot \tan \theta} \right)^{1/3} \quad (6)$$

$$\theta = \sin^{-1} \left( \frac{\delta}{OL} \right) \quad (7)$$

where  $g$  is gravitational acceleration  $\rho_A$  is aerial density,  $T_h$  is thickness of fabric,  $\rho$  is fabric volumetric density,  $\theta$  is the angle created between the  $\delta$  and overhang length ( $OL$ ), and finally  $c$  is bending length. Peirce first introduced the concept of the bending length as the length of fabric that will bend under its own weight during the cantilever test [22]. It mathematically relates the overhang length to the fabric’s flexural stiffness. The relationship between the bending length and the overhang length (equation 6) was developed based on elastic theory and corrected with

empirical data. About twenty measurements for each sample at each  $OL$  were tested and the average value of bending moduli was taken.

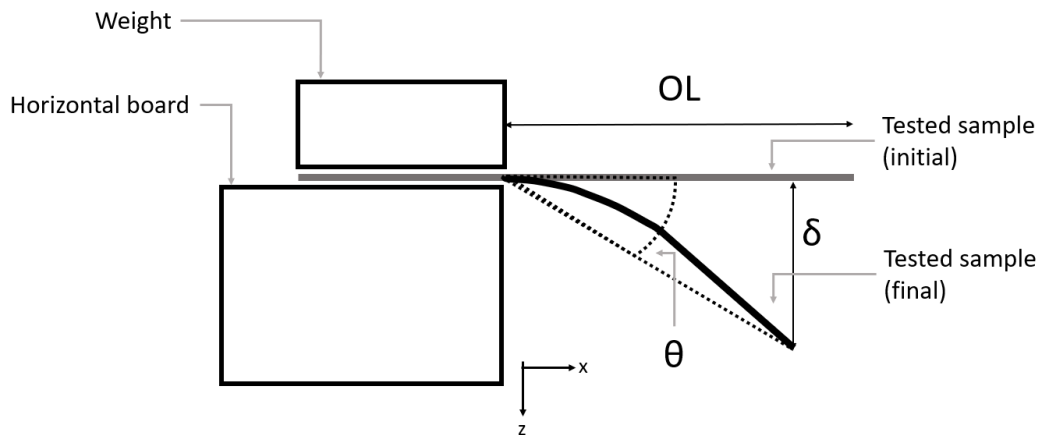


Figure 3. Bending behaviour characterization test setup

## 2.4 PAM-FORM Software

The commercial tool PAM-FORM from ESI Group was used to simulate the fabric draping behaviour. This software has a wide range of applications including rigid mould stamping, rubber pad forming, thermoforming and flexible membrane forming [19]. The simulation predicts the final fibre orientation, the thickness distribution, the optimum flat pattern and the preforming defects at both ply and laminate levels [19]. The software can perform simulations for both fabrics and unidirectional prepreg materials. Non-linear elasto-plastic material properties can be modelled by adding temperature, strain, strain-rate, pressure, viscosity dependencies [19]. The material data card in PAM-FORM requires the fabric shear, bending, and tensile properties in the warp and weft directions.

## 3 Results and Analysis

### 3.1 Picture-Frame Result Analysis

Figure 4 shows the variation of the shear stress as a function of the fabric shear angle for TG15N samples tested in the warp and weft directions. It can be observed that the shear behaviour of the NCF fabric is the same in both directions. Similar results were obtained for TG33N and SG33N. Therefore, the subsequent samples were only tested in the warp direction. Figure 5 compares the shear behaviour of the three tested NCF. From the shear stress – strain curves, the NCF locking angle can be determined at the intersection of the two tangents of the curve inflection and the values are reported in Figure 5. The locking angles (in rad) for TG15N, SG33N, and TG33N were measured as 0.95, 0.85 and 0.76 respectively.

There are three ways to implement shear properties of fabric in PAM-FORM: constant shear modulus, variable shear moduli post and pre locking angle, or shear stress – strain curve. The later method was chosen to implement the measured shear stress - strain properties from Figure 5 in PAM-FORM.

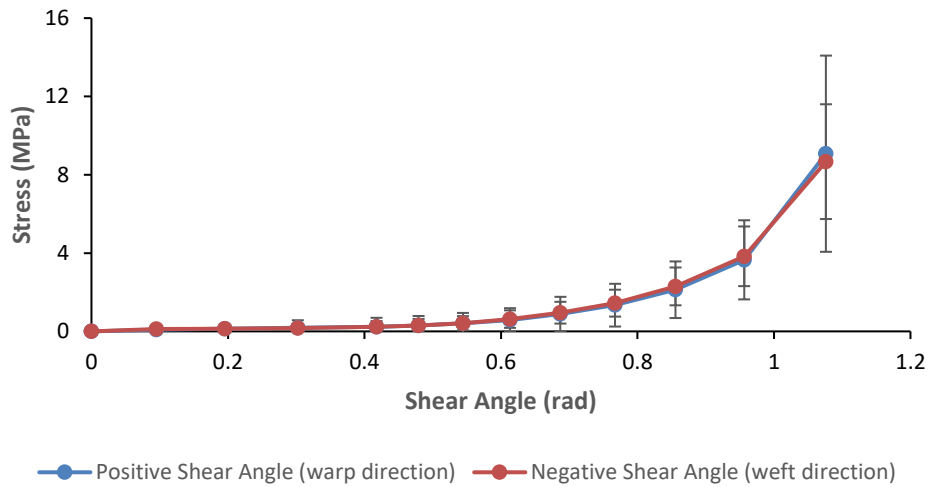


Figure 4. Shear behaviour for TG15N samples tested in positive and negative warp orientation.

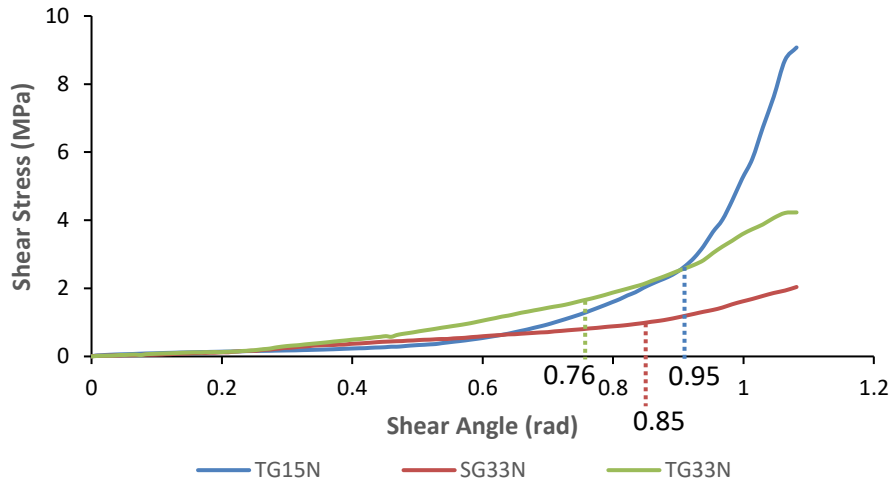


Figure 5. Comparison of the shear behaviour measured for TG15N, SG33N, and TG33N with locking angles.

### 3.2 Shear Behaviour Validation

The validations of shear properties for each material were performed with a single element simulation with the boundary conditions shown in the Figure 6: three imposed displaced nodes (arrows) and one fixed node. The imposed displacement of the top node in the vertical direction corresponds to the crosshead displacement of the load cell. The two imposed displacements of the side nodes in diagonal directions were kinematically coupled with the vertical displacement. The single element simulation allowed to keep the four edges straight while getting the representative reaction force and displacement of the top node. The reaction force and the displacement of the top node were compared with the picture-frame experimental force-displacement curves obtained for each material. Figure 7 compares the experimental and numerical force-displacement curves for the three tested materials. Good correlations with very high confidence level can be observed for all three materials with  $R^2$  value above 0.96.

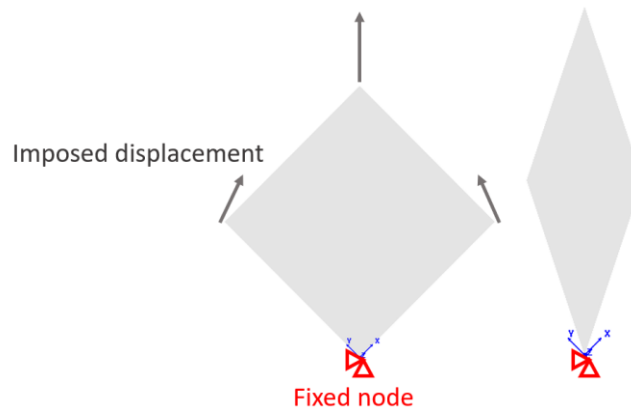


Figure 6. One element picture-frame validation simulation with boundary conditions (left) and deformed shape (right)

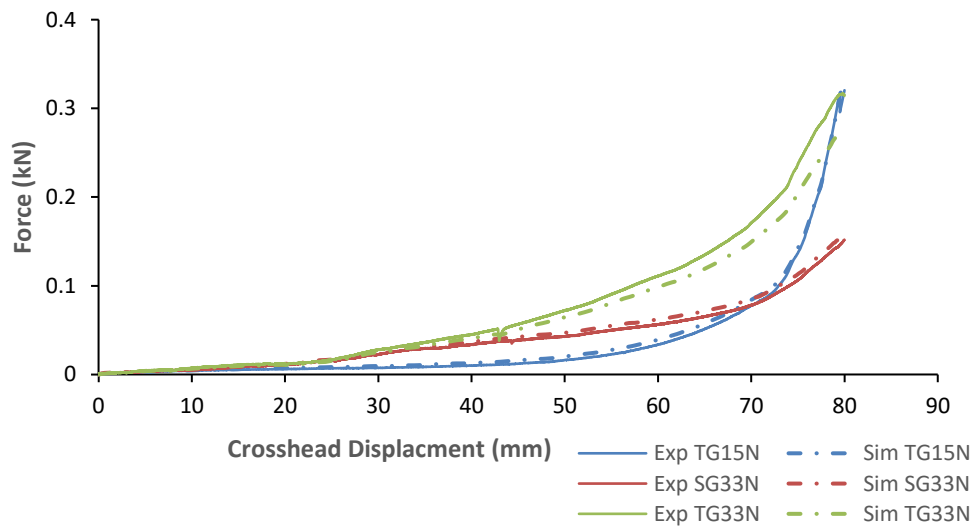


Figure 7. Comparison of force and crosshead displacement between simulation and experimental results for the picture frame test

### 3.3 Bending Cantilever Result Analysis

Figure 8 shows the bending modulus results at different overhang lengths for both warp and weft directions. No significant variation of the bending modulus with the overhang lengths was observed. Thus, the average bending modulus and flexural rigidity values for each material were computed and reported in Table 2. Contrary to TG15N and TG33N, the bending behaviour of SG33N in the warp and weft direction is significantly different. Lower bending modulus was measured in the warp direction due to thermoplastic binder stitch. From these bending properties of the three NCF materials, it can be assumed that TG15N will be more prone to wrinkles due to its high bending modulus, but easier to conform to complex geometry due to its low flexural rigidity.

There are two ways to implement bending properties of fabric in PAM-FORM: constant bending modulus or variable bending modulus in function of radius of curvature. In this work, the bending modulus value was implemented as a constant value (Table 2) for each material in both directions.

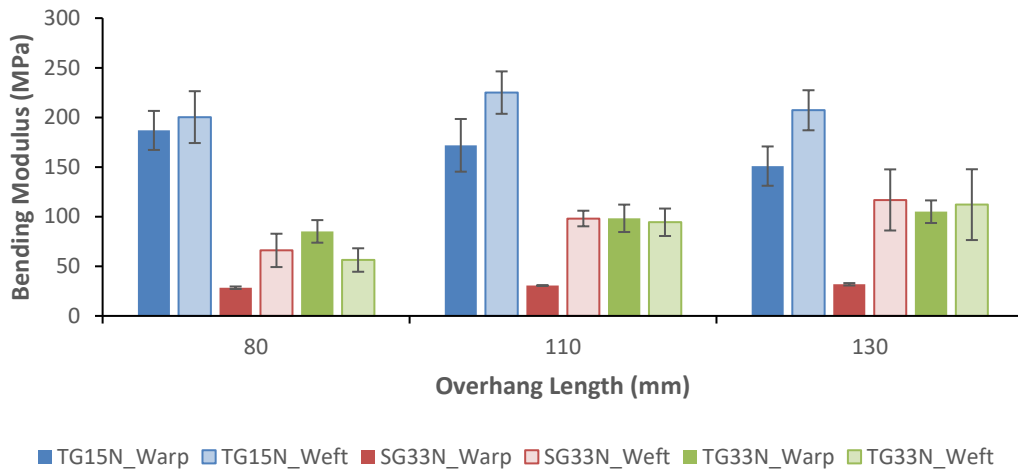


Figure 8. Bending modulus results at different overhang lengths and different directions.

Table 2. Average values of bending modulus and calculated flexural rigidities.

	Bending Modulus (MPa)		Flexural Rigidity ( $10^{-3}$ N·m)	
	Warp	Weft	Warp	Weft
<b>TG15N</b>	0.161	0.216	1.29	1.60
<b>SG33N</b>	0.031	0.107	2.17	7.15
<b>TG33N</b>	0.102	0.103	4.17	4.09

### 3.4 Bending Behaviour Validation

The bending properties were validated by modelling the bending cantilever test in PAM-FORM as shown in Figure 9. A rectangular model was created with a fixed edge on one side. Gravitational force was applied to the rest of the elements. From the simulation, the curvature profile was extracted and compared to the experimental curvature profile obtained with the cantilever test. Comparison between experimental and simulation bending curvature profile obtained is shown in Figure 10. Good correlations for all three materials can be observed with a high  $R^2$  values of over 0.97.

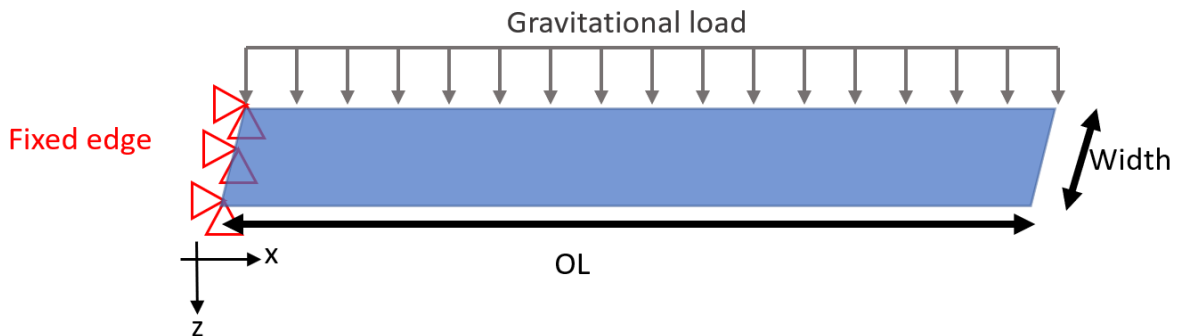


Figure 9. Load and boundary conditions of PAM-FORM cantilever test simulation

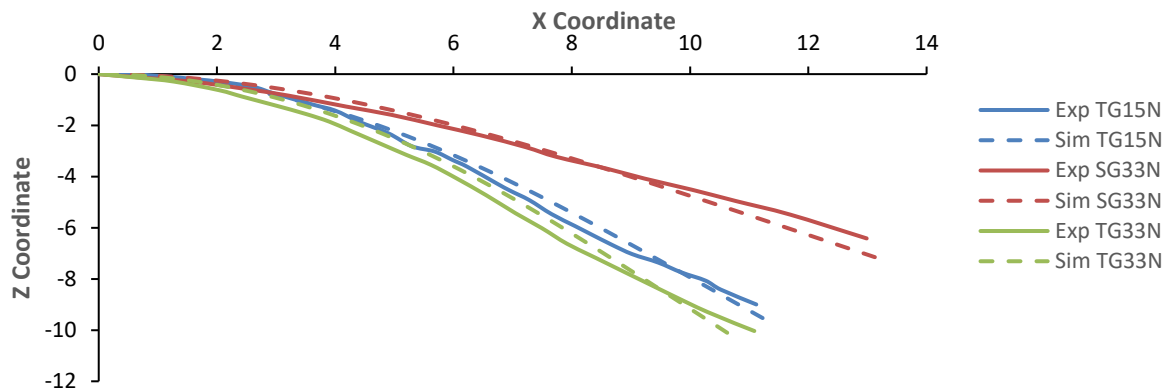


Figure 10. Experimental and numerical comparison of the bending curvature of NCF reinforcements subjected to the cantilever test.

## 4 CONCLUSION

In this study, the shear and bending properties of NCF (TG15N, TG33N, and SG33N) reinforcements were characterized and implemented in PAM-FORM preforming software. NCF material data cards were validated by modelling the shear and bending characterization tests and comparing experimental and numerical results. Good correlations were obtained for both behaviours. From those characterization tests, TG15N seems to have the best drapability properties for both shear (until 0.65 rad) and bending properties. It may be less susceptible to have wrinkles during preforming compared to the other two materials. This material would be suitable for preforming of complex geometry which has high curvature. SG33N also has a high locking angle and relatively low flexural rigidity in the warp direction. By placing the fabric such that the warp direction is in parallel to curvature's tangential direction, this material could also be a great option for preforming complex geometry. The thermoplastic binder integrated in its architecture could be directly used as fabric binder to simplify the preforming process.

As future work, the developed and validated material data cards will be used to model the preforming behaviour of NCF preform for complex 3D geometries. Preforming simulations will be used to determine optimal flat pattern, and predict preforming defects such as wrinkles, bridging and shear and reduce trial-and-error preforming tests. Different preforming technologies, such as matched-tool, membrane forming or vacuum bagging, will be also model to assess the best process for preform geometrical accuracy and manufacturing efficiency.

## 5 ACKNOWLEDGEMENTS

The authors would like to acknowledge the financial support from the Natural Sciences and Engineering Research Council of Canada (NSERC), PRIMA Quebec, Texonic <sup>Inc.</sup> and IND Experts. The authors would also like to thank Patrick Gagnon from National Research Council of Canada (Boucherville, QC) for his help during picture-frame tests, members of Centre Technologique en Aérospatiale - Secteur Composites et Matériaux Avancés (St-Hubert, QC) for providing the bending cantilever setup and Arnaud Dereims from ESI Group for his precious support for PAM-FORM software.

## 6 REFERENCES

- [1] D. Mattsson, "Mechanical performance of NCF composites," PhD, Applied Physics and Mechanical Engineering, Luleå tekniska universitet, Luleå, 2005.
- [2] J. Viisainen and M. Sutcliffe, "Characterising the variability in wrinkling during the preforming of non-crimp fabrics," *Composites Part A: Applied Science and Manufacturing*, vol. 149, p. 106536, 2021.
- [3] M. Nishi, T. Hirashima, and T. Kurashiki, "Textile composite reinforcement forming analysis considering out-of-plane bending stiffness and tension dependent in-plane shear behavior," in *Proceedings of the 16th European Conference On Composite Materials, Seville, Spain, 2014*.
- [4] U. Mohammed, C. Lekakou, L. Dong, and M. Bader, "Shear deformation and micromechanics of woven fabrics," *Composites Part A: Applied Science and Manufacturing*, vol. 31, no. 4, pp. 299-308, 2000.
- [5] K. Vanclooster, S. V. Lomov, and I. Verpoest, "Experimental validation of forming simulations of fabric reinforced polymers using an unsymmetrical mould configuration," *Composites Part A: Applied Science and Manufacturing*, vol. 40, no. 4, pp. 530-539, 2009.
- [6] D. Lussier and J. Chen, "Material characterization of woven fabrics for thermoforming of composites," *Journal of Thermoplastic Composite Materials*, vol. 15, no. 6, pp. 497-509, 2002.
- [7] A. Mallach, F. Härtel, F. Heieck, J.-P. Fuhr, P. Middendorf, and M. Gude, "Experimental comparison of a macroscopic draping simulation for dry non-crimp fabric preforming on a complex geometry by means of optical measurement," *Journal of Composite Materials*, vol. 51, no. 16, pp. 2363-2375, 2017.
- [8] J. Cao *et al.*, "Characterization of mechanical behavior of woven fabrics: experimental methods and benchmark results," *Composites Part A: Applied Science and Manufacturing*, vol. 39, no. 6, pp. 1037-1053, 2008.
- [9] P. Boisse, N. Hamila, E. Vidal-Sallé, and F. Dumont, "Simulation of wrinkling during textile composite reinforcement forming. Influence of tensile, in-plane shear and bending stiffnesses," *Composites Science and Technology*, vol. 71, no. 5, pp. 683-692, 2011.
- [10] S. Bel, P. Boisse, and F. Dumont, "Analyses of the deformation mechanisms of non-crimp fabric composite reinforcements during preforming," *Applied Composite Materials*, vol. 19, no. 3, pp. 513-528, 2012.
- [11] S. Chen, O. McGregor, L. Harper, A. Endruweit, and N. Warrior, "Defect formation during preforming of a bi-axial non-crimp fabric with a pillar stitch pattern," *Composites Part A: Applied Science and Manufacturing*, vol. 91, pp. 156-167, 2016.
- [12] S. Allaoui *et al.*, "Experimental and numerical analyses of textile reinforcement forming of a tetrahedral shape," *Composites Part A: Applied Science and Manufacturing*, vol. 42, no. 6, pp. 612-622, 2011.
- [13] E. de Bilbao, D. Soulat, G. Hivet, and A. Gasser, "Experimental study of bending behaviour of reinforcements," *Experimental Mechanics*, vol. 50, no. 3, pp. 333-351, 2010.
- [14] K. A. Fetfatsidis, D. Jauffrès, J. A. Sherwood, and J. Chen, "Characterization of the tool/fabric and fabric/fabric friction for woven-fabric composites during the thermostamping process," *International journal of material forming*, vol. 6, no. 2, pp. 209-221, 2013.
- [15] TG-15-N. Texonic INC, 2019.
- [16] SG-33-N. Texonic INC, 2019.
- [17] TG-33-N. Texonic INC, 2018.
- [18] M. Karaki, R. Younes, F. Trochu, and P. Lafon, "Progress in experimental and theoretical evaluation methods for textile permeability," *Journal of Composites Science*, vol. 3, no. 3, p. 73, 2019.
- [19] PAM-FORM User's Guide. ESI Group, 2020.
- [20] L. Krishnappa, J.-H. Ohlendorf, M. Brink, and K.-D. Thoben, "Investigating the factors influencing the shear behaviour of 0/90° non-crimp fabrics to form a reference shear test," *Journal of Composite Materials*, vol. 55, no. 20, pp. 2739-2750, 2021.
- [21] GetData Graph Digitizer. [Online]. Available: <http://getdata-graph-digitizer.com/index.php>
- [22] F. T. Peirce, "26—The "handle" of cloth as a measurable quantity," *Journal of the Textile Institute Transactions*, vol. 21, no. 9, pp. T377-T416, 1930.